HAVE 2008 - IEEE International Workshop on
Haptic Audio Visual Environments and their Applications
Ottawa, Canada, 18-19 October 2008

Haptic and Visual Rendering of Virtual Bone Surgery: A Physically Realistic Voxel-Based Approach

M. Arbabtafti[1], M. Moghaddam[1], A. Nahvi[2], M. Mahvash[3], A. Rahimi[4]

[1]Department of Mechanical Engineering
Tarbiat Modares University
P.O. Box 14115-111, Tehran, Iran
Phone: +98 021 82883358, Fax: +98 021 82883358, E–mail: arbab, mogaddam@modares.ac.ir.

[2]Department of Mechanical Engineering
K.N. Toosi University of Technology
Mirdamad St., Tehran, Iran
Phone: +98 021 84063234, Fax: +98 021 88674748, E–mail: nahvi@kntu.ac.ir

[3]Department of Aerospace and Mechanical Engineering
Boston University
Boston, USA
Phone: +1 0617 5165477, Fax: +1 0617 5165477, E–mail: mahvash@bu.edu

[4]Department of Electrical and Computer Engineering
Tehran University
Tehran, Iran
Phone: +98 021 88027757, Fax: +98 021 88633029, E–mail: ab.rahimi@ece.ut.ac.ir

Abstract – *A physics-based haptic surgical simulator for bone surgery is presented. The simulator uses voxels to represent virtual bones obtained from CT or MRI data. We use a analytical force model of bone milling process to calculate interaction forces. The analytical model considers the interior structure and the mechanical properties of heterogeneous bone. A real-time voxel-based implementation of the model is described using a 3DOF haptic device. 3D texture-based volume rendering is used to display the bone and to visually remove bone material due to drilling in real-time.*

Keywords – *Physics-Based Simulation, Bone Surgery Simulator, Multi-rate Haptic Rendering, Voxel-Based Simulation, Virtual Reality.*

I. INTRODUCTION

Bone milling is used in many surgical procedures including otologic surgery, orthognathic surgery, and dentistry. During bone milling, a part of a bone is removed by a series of spherical burrs rotating in a high speed. Haptic simulators can help surgeons to learn bone surgery procedures in an efficient way outside the operating room [1].

Over the past decade, a number of approaches for bone surgery simulation have been presented. Temporal bone surgery simulation was done at Ohio Sate University using a point-based collision detection approach [2]. Petersik et al. [3] presented a haptic rendering algorithm for bone cutting process based on a multi-point collision detection approach. Morris et al. [4] made some haptic rendering improvements to [3] by voxelizing the tool tip as well as the bone volume. Agus et al. [5] applied Hertz's contact theory to determine the elastic force of burr bone interaction in their temporal bone surgery simulation. Friction force that opposes the burr rotation was also included. Wang et al. [6] presented a dental surgery simulation system using a point-based force model. Kim et al [7] introduced a single point of the virtual tool for force computation based on an offset surface in their haptic dental simulation system. Yau et al. [8] developed a dental training system and developed smooth force interaction with the haptic device using an octree-based adaptive voxel model connected by a matrix of spring network at the edge of bone voxels.

The haptic rendering methods presented above are mostly not physics-based. But, to create realistic surgical simulators, a high-fidelity approach is to calculate forces from physics-based models [9]. In our previous work [10], an analytical force model was developed to predict the cutting forces of bone milling process.

In this paper, a real-time voxel-based implementation of our previous physics-based model [10] is described and tested on a haptic device. The bone volume is extracted directly from the CT data as a contiguous array of voxels. Our volumetric model can perceive the interior structure and the mechanical properties of heterogeneous bone. Hardware accelerated 3D texture-based volume rendering is used to display the bone and to visually remove the bone material due to drilling simulation in real-time. Stability of the contact is achieved through

a sample-estimate-hold approach [11] in order to remove the excess energy in the tool-bone interaction.

II. CUTTING FORCE MODEL

Fig. 1(a) shows a spherical tool utilized in almost all bone cutting applications. The geometry and the cutting forces on the spherical milling cutter are shown in Fig. 1 (b). The force on each cutting tool element has three components (dF_t, dF_r and dF_a). dF_t is the main cutting force due to the bone orthogonal cutting. dF_r is a frictional force on the rake surface. dF_a is another frictional force component due to the effect of helix angle of cutting edges [10]. Other parameters of Fig. 1 (b) will be explained shortly.

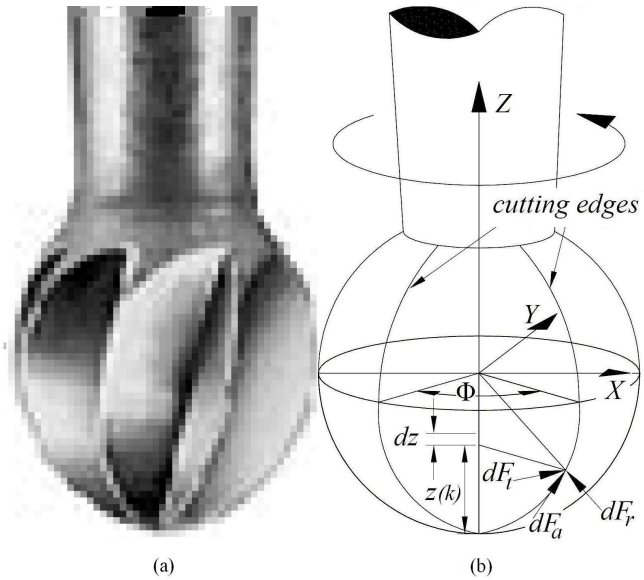

Fig. 1. (a) Spherical burr bone tool, (b) Tool geometry and cutting forces on spherical burr bone tool.

The total force expressed in the Cartesian coordinate system is then obtained by multiplying by the spherical transformation matrix T:

$$\begin{bmatrix} F_x(j) \\ F_y(j) \\ F_z(j) \end{bmatrix} = \left\{ \sum_{i=1}^{N_\phi} \sum_{k=1}^{N_z} T(i,j,k) \begin{bmatrix} K_t \\ K_r \\ K_a \end{bmatrix} t(i,j,k)dz \right\} \tag{1}$$

where N_ϕ is the number of cutting edges and N_z is the number of the discretized elements of a cutting edge. The height of each element is dz as shown in Fig. 1(b). Assuming N_θ time intervals as each cutting edge travels the angular spacing of ϕ, we would like to calculate the force at the jth fraction of ϕ. The higher the N_θ, the more accurate our results will be. $t(i,j,k)$ is the chip thickness in a cutting edge i at the jth fraction of ϕ. Chip thickness is the most dominant factor in computation of the cutting forces and represented voxel-based in the next section. However, the chip thickness can be derived analytically and is affected by the feed rate of the tool [10]. The cutting force coefficients K_t and K_r are obtained from a set of orthogonal bone cutting tests [12],[13] and are equal to $230N/mm^2$ and $40N/mm^2$. K_a is a fraction of K_r to take into account the effect of the helix angle of the cutting edge and is equal to $20N/mm^2$.

III. VOXELIZED FORCE MODEL

A voxel-based force model is needed for the purpose of implementation. Fig. 2 shows the bone spherical tool in two successive positions - dashed and solid - where the spherical tool moves from the first position to the second position. As equation (1) is essentially discrete, only the chip thickness needs to be represented voxel-based to include all voxels between successive positions [10]. The chip thickness is determined proportional to the number of bone voxels located inside of the spherical tool. First, the voxels in the intersection region of the bone volume and the spherical tool are identified. Secondly, the Cartesian coordinates of each voxel $v(X,Y,Z)$ are transformed into the cylindrical coordinates of the tool $v(r,\Psi,z)$ as shown in Fig. 2. Finally, the number of voxels are counted in each rotational angle increment and height increment, and then normalized based on the feed and assigned to the chip thickness. The simulation results showed a close force correlation between the voxel-based method and an analytical force model [10].

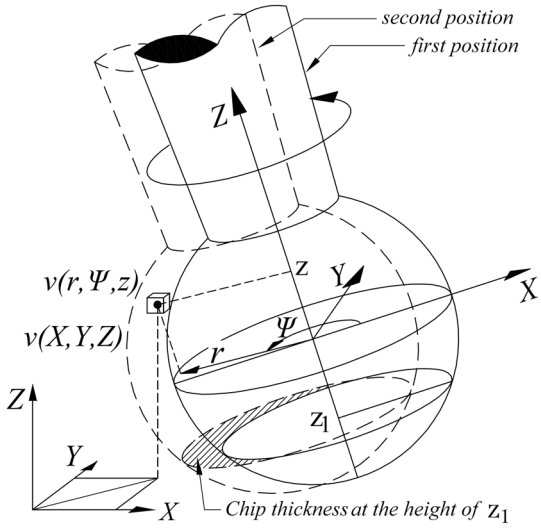

Fig. 2. Voxel-based chip thickness evaluation.

It is important to elaborate that because of the high spinning speed of the tool, each cutting edge travels a large angular distance at each $1msec$ servo period of the haptic loop. We have shown in our previous paper [10] that the total cutting force changes significantly as the angular location of the cutting edges change. If ω represents the angular velocity of the spherical tool in rpm, it takes $60/\omega$ seconds to take one turn, and $\Delta t = 60/(N_\phi \omega)$ seconds to travel between two successive cutting edges. For a typical spinning speed of 10,000 rpm

and 6 cutting edges, we have $\Delta t = 1msec$ $(1kHz)$. So, calculation of the accurate cutting force in 10 time intervals (i.e. $N_\theta = 10$) would require a servo rate of $10kHz$. Since $1kHz$ in the haptic loop is sufficient for the perception of users, we need to take the average of forces found in equation (1), rather than applying the accurate force for every degree of the tool angular location :

$$\begin{bmatrix} F_x \\ F_y \\ F_z \end{bmatrix} = \left\{ \sum_{i=1}^{N_\phi} \sum_{k=1}^{N_z} \sum_{j=1}^{N_\theta} T(i,j,k) \begin{bmatrix} K_t \\ K_r \\ K_a \end{bmatrix} t(i,j,k) dz \right\} / N_\theta \tag{2}$$

IV. REAL-TIME HAPTIC VISUAL RENDERING

Haptic rendering requires at least 1 kHz force display to keep the system stable, while displaying smooth and realistic forces. In order to keep this extreme computational requirement, we used a multi-rate strategy for haptic rendering of the forces. Actually the haptic rendering comprises two threads run in parallel: the $simulation\ thread$ and the $haptic\ thread$. Our $simulation\ thread$ running at about 100 Hz is responsible for updating the force components according to the model. The haptic thread running at 1 kHz deals with the multi-rate strategy and calculates forces by interpolating between two successive forces obtained in the $simulation\ thread$.

In the graphic loop running at about 20-30 Hz, a direct volume rendering method (3D texture-based) is used to display the bone and to visually remove the bone material.

A. Real-time Haptic Implementation of the Voxel-Based Model

The Voxel-Based model is implemented in the low-rate $simulation\ thread$ of the haptic loop. First, the chip thickness has to be determined. As mentioned in Section III, the chip thickness is proportional to the number of voxels in the intersection region of the bone volume and the spherical tool. Thus a voxel-based collision detection algorithm is necessary to identify voxels in that region.

In voxel-based formats, collision detection is more straightforward than surface-based graphical formats. Moving objects in virtual space involves shifting objects in a large memory array of voxels and detecting collisions among them by checking the new memory locations of each object voxels to see if they are already occupied [14].

Consequently, similar to [4] in our collision detection implementation, the volume of the spherical tool is voxelized too. Also, the bone volume extracted from CT or MRI data is a contiguous array of voxels.

Figure (3) shows the flow chart of the $simulation\ thread$. First, the position of the center of the spherical tool (x_0, y_0, z_0) is derived from forward kinematics of the haptic robot. Then, for each voxel of the tool (x_1, y_1, z_1), collision is checked with the bone volume. The stiffness value of each voxel is set from CT data. The Cartesian coordinates of each voxel in the intersection region are then transformed into the cylindrical coordinates of the tool (as shown in Fig. 2). This cylindrical coordinate is derived from the forward kinematics of the haptic robot. We use a 2D array $th[\Psi, z]$ to store the chip thickness by adding up the voxel stiffness in each angle Ψ and height z. The force components (Fx, Fy, Fz) are calculated according to chip thickness matrix $(th[\Psi, z])$ using equation (2). These forces are in the tool Cartesian coordinates and must be transformed to the global Cartesian coordinates for rendering.

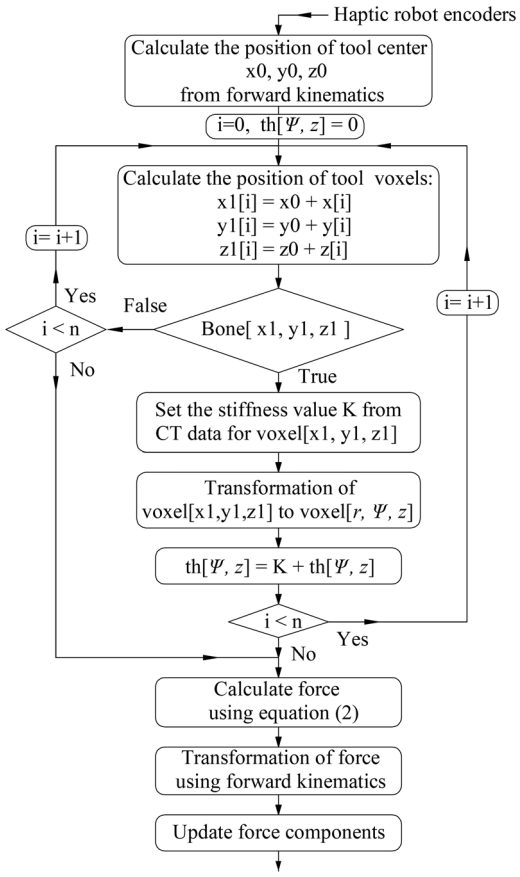

Fig. 3. $Simulation\ thread$ flow chart.

This volumetric method allows quantification of the mechanical properties of the interior structure of the bone. As bone is a heterogeneous material, its mechanical stiffness varies in different regions of the volume. The cutting force is proportional to the strength of the bone material as well as the chip thickness. So, we can assume a thicker chip for a stronger material. Therefore, we add up the stiffness value K of each voxel to the chip thickness as shown in the flow chart of Fig (3). It means every voxel has its contribution to the $th[\Psi, z]$ matrix according to its strength value. Fortunately, MRI and CT Images specify bone density at each voxel, which is nearly an indicator of the bone strength.

B. Graphical Rendering Loop

Visualization is implemented using direct volume rendering methods [15], [16] rather than indirect methods [17]. Specifically, hardware-accelerated 3D texture based volume rendering is performed [15] in OpenGL API in order to render the CT bone data. The most important feature of the method is that it makes direct use of volumetric data with little preprocessing and high frame rates.

Illumination and shading provides a more realistic visual appearance of 3D models and improves the visual depth cue significantly. In our implementation, we use reflection model of Phong [18] but the specular lighting component is omitted for simplicity.

In order to shade a 3D object, a light source (L1) must be defined, and normal vector must be calculated for all surface voxels of the 3D model. A voxel is a surface voxel if at least one of its 26 neighboring voxels is outside the 3D object. When a surface voxel is identified, a normal vector is calculated as the normalized sum of all the gradient-weighted unit vectors of its outside neighbors.

We considered a fixed position for each light relative to the scene. But, a moving light relative to the scene, would require calculation of the texture color continuously, which decreases the performance of the algorithm.

When the user performs the drilling operation, the surface of the virtual bone, e.g. a tooth, should be modified according to the shape of the applied tool. The process of carving involves positioning the tool volume with respect to the object in 3D space and performing a Boolean subtraction between these two volumes. In our system, a set of spherical tools with different diameters (1-5mm) are available to the user.

Furthermore, since a typical sculpting action only modifies a small region of the object volume, it is sufficient to identify the surface voxels in a small local area around the affected region. Then we compute and change the RGB values of only these surface voxels in the 3D texture. Consequently, interactive rendering speed is achieved.

Our bone volume was extracted directly from a mandible CT data. We used some threshold to isolate bone regions from other soft tissue. In our implementation, the voxel size is 0.1 mm. As CT images at best have the voxel size of $0.2\times0.2\times0.4$mm, a preprocessing step is necessary to reach a smaller size. So, we refined the CT data to produce isotropic voxels, 0.1mm on each side.

Fig (4) shows the graphical rendering of a dental CT scan of size $512\times512\times128$. Part (a) shows the original data set and part (b) shows the drilling procedure on the second tooth from the right end. The user removes carious lesions on the virtual tooth by using a spherical drill tool (1.5mm in diameter) and making a hole of about 4.5mm in diameter. The whole scene can rotate and move in real time as well.

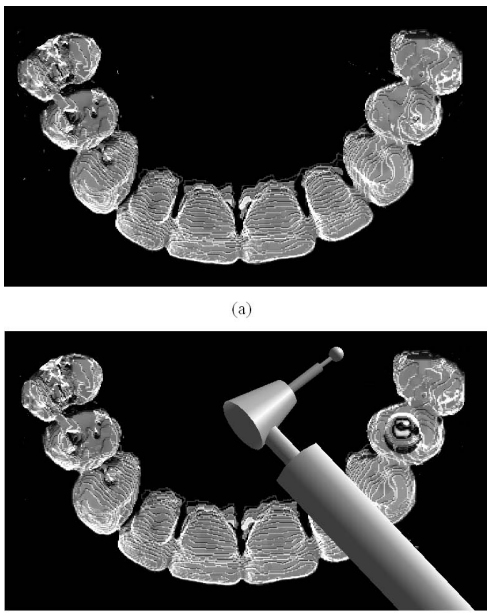

(a)

(b)

Fig. 4. The graphical rendering of a dental CT scan of size $512\times 512 \times 128$. Part (a) shows the original data set and part (b) shows the drilling procedure on the second tooth from the right end.

V. EXPERIMENTS

A. Experimental Setup

The experimental setup includes a PHANToM Omni device as the haptic interface. It provides six-DOF tracking and three-DOF force feedback. It also includes a CRT monitor for showing the teeth and the virtual tool.

The haptic and graphic loops run on separate PCs. The first PC is a 3.0 GHz Pentium 4 with 512 MB RAM that runs the high-frequency tasks of the haptics. Three threads run in parallel in this PC: the first thread, which we called $simulation\ thread$ in Section IV, reads six encoders and calculates force components at 100 Hz; the second thread, which we called $haptic\ thread$ in Section IV, interpolates force components of the first thread and runs at 1kHz; and the third thread sends encoder values as data packets to the second PC at 30 Hz via a 100 Mbit Ethernet link with TCP/IP protocol.

The second PC is a 3.0 GHz Pentium 4 with 1 GB RAM and an NVIDIA GeForce 3 Ti 500 graphics card. Two threads run in parallel in this PC: one thread updates the graphics scene at 30 Hz; the second thread receives encoder values from the first PC at 30 Hz.

B. Experimental Results

We chose a polishing operation to implement our experiments. Polishing has two advantages for us: 1. Polishing operation is performed in almost all bone surgery procedures, e.g.

temporal and dental bone surgery [5]; 2. The results of force components of our model in the polishing operation is easily comparable to those of point-based models.

Figure 5 shows a surface polishing action where a virtual cubic bone volume is dissected by a polishing movement of a spherical tool of 5 mm in diameter. This virtual cube has all the properties of bone material, i.e. $K_t = 230N/mm^2$, $K_r = 40N/mm^2$, and $K_a = 20N/mm^2$. The bone cube is homogeneous and all voxels have the same stiffness values. The voxel size is 0.1 mm and over 60000 voxels were used for the 5-mm spherical tool.

Ellis et al. proposed a numerical method to minimize the energy infusion by modifying the regular zero-order hold value of the force [11]. They computed the force based on the previous zero-order representation and called it the sample-estimate-hold approach. We used their method in order to stabilize the contact force.

Figure 6 shows the cutting depth below the surface level versus time during the sliding motion of the polishing procedure. The user held the end point of the haptic device and moved the spherical tool by a sliding speed of about 6 mm/s, and traveled a path of about 40 mm long in about 7 seconds. The tool cut the bone as much as 3.5 mm.

Figure 7 plots the reaction force components of the bone by our model in three directions. The reaction force components of the point-based model are also shown. The point-based model is: $F_x = 0; F_y = 0; F_z = k * z$. In other words, the point-based model is a linear spring acting perpendicular to the surface of the bone.

Comparing figures 6 and 7, we realize that an increase in the depth of cut leads to an increase in all three force components in our model; i.e. a rise in the cutting depth has a corresponding rise in the force plots.

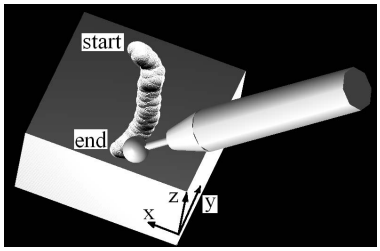

Fig. 5. Surface polishing of a virtual cubic bone by a 5-mm spherical tool operated by a user holding the stylus of the PHANToM Omni device.

VI. DISCUSSION

An important problem in the field of force-reflecting systems is the mechanical instability of the contact, especially against rigid objects. The main possible source of poor force performance is low-rate haptic rendering [19], which we overcame by a multi-rate rendering approach. Adding a virtual

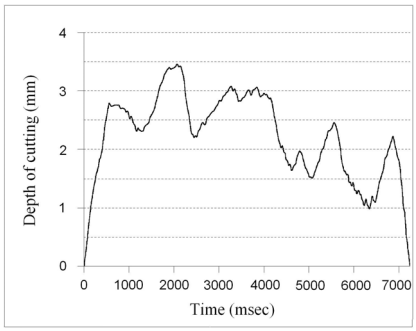

Fig. 6. Depth of the spherical tool below the surface level as a function of time for the test case shown in figure 5.

damper to the model would be typically a good solution to increase the stability of the rigid body contact [20], even though it may significantly decrease the fidelity of the reflected forces. In our experiments, we applied the sample-estimate-hold approach [11] to stabilize the contact as mentioned in Section V. B. Had we not used this, the result would have been as shown in figure 8 which is almost unstable.

In this polishing operation, other factors such as tool orientation and sliding speed are not constant during the procedure. These factors affect force components during the cutting action according to the our force mode - a nonlinear effect for the tool orientation and a linear effect for the sliding speed. That is why our force components are not proportional to each other in figure 7. For example, in the first rise of figure 7, Fx and Fy are 0.3 N and 0.35 N, while in the second rise, Fx and Fy are 0.3 N and 0.7 N, respectively.

As mentioned in our previous paper [10], the chip thickness is affected by the number of cutting edges and the tool angular velocity. So, in our model, force components decrease as the number of teeth or the spindle speed increase.

VII. CONCLUSION AND FUTURE WORKS

A haptic surgery simulator for bone milling was presented. We used a voxel-based method to represent bone volume and bone properties. A real time implementation of the voxel based model for bone machining by spherical tool was presented [10].

The bone volume was extracted directly from the CT data. Our volumetric model can perceive the interior structure and the mechanical properties of heterogeneous bone using these data. Hardware accelerated 3D texture-based volume rendering was used to display the bone and to visually remove the bone material due to drilling simulation in real-time.

Stability of the contact was achieved through a sample-estimate-hold approach [11] in order to remove the excess induced energy of the tool-bone interaction.

In the next step we plan to evaluate and tune our simulation system with the help of some expert surgeons.

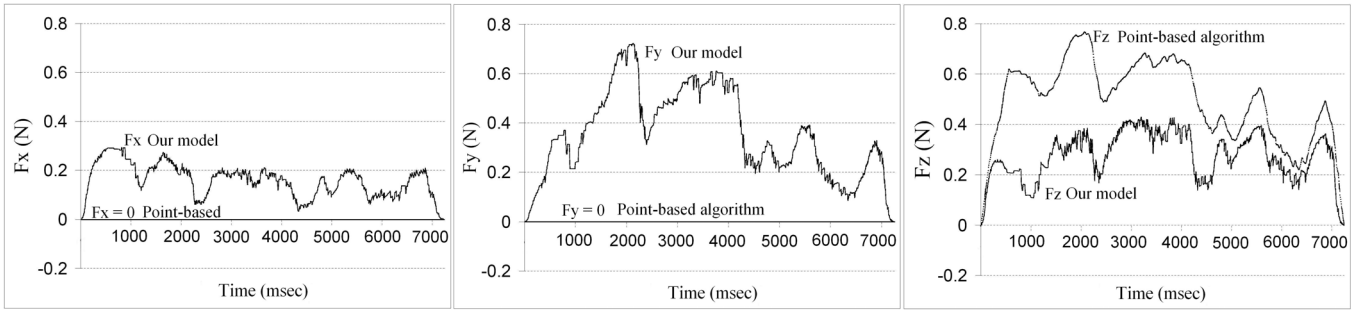

(a) (b) (c)

Fig. 7. The reaction force components of bone polishing procedure in three directions: (a) Fx, (b) Fy, (c) Fz.

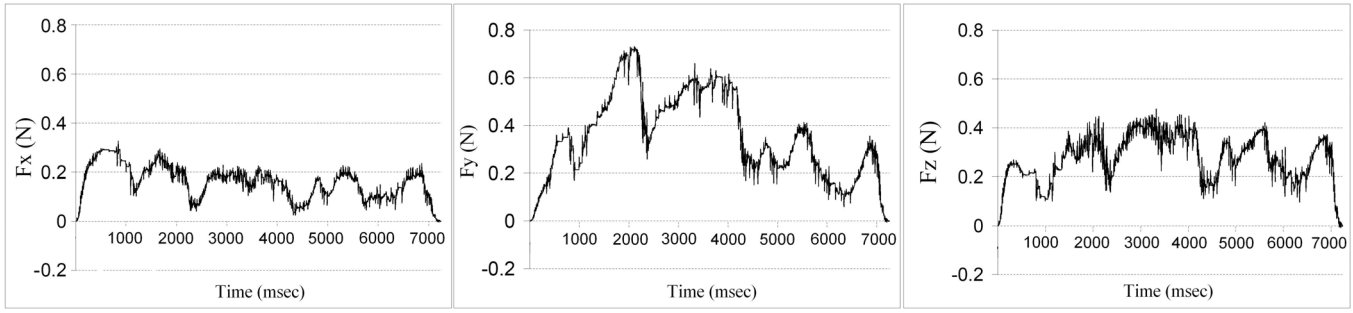

(a) (b) (c)

Fig. 8. The reaction force components of bone polishing procedure without the sample-estimate-hold approach in three directions: (a) Fx, (b) Fy, (c) Fz.

ACKNOWLEGMENT

We would like to express our gratitude to Mr. M. Alinaghizadeh at Noor Medical Imaging Center of Tehran for providing us with dental CT scans. We Also thank Mr. H. Khakpoor and Mr. H. Mohtasham for computer programming assistance.

[1] T. R. Jasinevicius, M. Landers, S. Nelson, A. Urbankova, "An Evaluation of two dental simulation systems: Virtual reality versus contemporary non-computer-assisted," *J. Dent. Educ.*, vol. 68, no. 11, pp. 1151–1162, November 2004.

[2] J. Bryan, D. Stredney, G. Wiet, D. Sessanna, "Virtual Temporal Bone Dissection: A Case Study," *Proc. of IEEE Visualization*, pp. 497–500, Oct. 2001.

[3] A. Petersik, B. Pflesser, U. Tiede, K. H. Hoehne, R. Leuwer, "Haptic Volume Intraction with Anatomic Modelsat Sub-Voxel Resolution," *Proc. 10th Symp. on Haptic Interfaces for Virtual Environment and Teleoperator Sys.*, pp. 66–72, 2002.

[4] D. Morris, C. Sewell, F. Barbagli, N. Blevins, S. Girod, K. Salisbury, "Visuohaptic Simulation of Bone Surgery for Training and Evaluation," *IEEE Computer Graphics and Applications*, vol. 26, no. 4, pp. 48–57, 2006

[5] M. Agus, A. Giachetti, E. Gobbetti, G. Zanetti, A. Zorcolo, "A Multiprocessor Decoupled System for the Simulation of Temporal Bone Surgery," *Computing and Visualization in Science*, vol. 5, no. 1, pp. 35–43, 2002.

[6] D. Wang, Y. Zhang, Y. Wang, Y. S. Lee, P. Lu, Y. Wang, "Cutting on Triangle Mesh Local Model-Based Haptic Display for Dental Preparation Surgery Simulation," *IEEE Trans. Visual. Comput. Graph.*, vol. 11, no. 6, pp. 671–683, 2005.

[7] L. Kim, S. H. Park, "Haptic Interaction and Volume Modeling Techniques for Realistic Dental Simulation," *Visual Computing*, vol. 22, pp. 90–98, 2006.

[8] H. T. Yau, C. Y.Hsu, "Development of a Dental Training System Based on Point-Based Models," *Computer-Aided Design & Applications*, vol. 3, no. 6, pp. 779–787, 2006.

[9] M. Mahvash, V. Hayward, "High Fidelity Haptic Synthesis of Contact with Deformable Bodies," *IEEE Comp. Graphics and App.*, vol. 24, no. 2, pp. 48–55, 2004.

[10] M. Moghaddam, A. Nahvi, M. Arbabtafti, M. Mahvash, "A Physically Realistic Voxel-Based Method for Haptic Simulation of Bone Machining," *Proc. of EuroHaptics 2008, LNCS 5024*, pp. 651–660, 2008.

[11] R. E. Ellis , N. Sarkar , M. A. Jenkins, "Numerical Methods for the Force Reflection of Contact," *ASME Transactions on Dynamic Systems, Modeling, and Control*, vol. 119, pp. 768–774, 1997.

[12] C. H. Jacobs, M. H. Pope, J. T. Berry, F. Hoaglund, "A Study of the Bone Machining Process–Orthogonal Cutting," *J. of Biomech.*, vol. 7, no. 2, pp. 131–136, 1974.

[13] C. Plaskos, A. J. Hodgson, P. Cinquin, "Modeling and Optimization of Bone-Cutting Forces in Orthopaedic Surgery," *MICCAI*, vol. 2878, pp. 254–261, 2003.

[14] S. F. Gibson, "Beyond Volume Rendering: Visualization, Haptic Exploration, and Physical Modeling of Voxel-based Objects," *in Visualization in Scientific Computing'95, eds. R. Scateni, J. van Wijk, P. Zanarini, Springer-Verlag, NY*, pp. 10–24, 1995.

[15] B. Cabral , N. Cam, J. Foran, "Accelerated Volume Rendering and Tomographic Reconstruction Using Texture Mapping Hardware," *Symposium on Volume Visualization*, pp. 91–98, 1994.

[16] J. T. Kajiya, B.P. Von Herzen, "Ray Tracing Volume Densities," *Proc. Siggraph 84*, pp. 165–173, 1984.

[17] W. E. Lorensen , H.E. Cline, "Marching Cubes: A High Resolution 3D Surface Construction Algorithm," *Proc. Siggraph 87*, pp. 163–169, 1987.

[18] B. T. Phong, "Illumination for Computer Generated Images," *Comm. of the ACM*, vol. 18, no. 6, pp. 311–317, 1975.

[19] J.E . Colgate, P.E. Grafing, M.C. Stanley, and G. Schenkel, Implementation of Stiff Virtual Walls in Force-Reflecting Interfaces," *Proc. IEEE Virtual Reality Annual Int. Symposium*, pp. 202–208, Seattle, 1993.

[20] R. J. Adams, B. Hannaford, "Stable Haptic Interaction with Virtual Environments, *IEEE Trans. Robo. Auto.*, vol. 15, no. 3, pp. 465–474, 1999.